Beam Focusing for Field-Emission Flat-Panel Displays

W. Dawson Kesling, *Student Member, IEEE*, and Charles E. Hunt, *Senior Member, IEEE*

***Abstract*—A combination of finite element and finite difference techniques have been used to simulate the performance of microfabricated gated field emitters for flat-panel display applications. The computer model has been verified against both analytic models and experimental data for unfocused devices and then applied to the study of focused structures for which sufficient models and data are not yet available. Quantitative results include electrode current-voltage characteristics and electron beam widths as a function of distance from the cathode. Practical issues such as visual image quality, electrical stress and fabrication complexity are considered to identify a practical design for use in conjunction with existing high-efficiency cathode ray tube phosphors. It is found that the addition of an integrated aperture electrode to focus the emitted electrons increases the cathode-gate drive voltage by about 30% over the case of unfocused emitters. A concentric electrode design results in only 15% increase and promises simpler fabrication. Both approaches demonstrate electron beam widths of tens of microns at anode distances of several millimeters, allowing for full-color resolution in excess of 100 lines per inch with proven color phosphors.**

I. Introduction

FLAT and thin replacements for the cathode ray tube (CRT) have been sought since the 1950's. Cathodoluminescent flat-panel displays represent one broad category of development, but have generally suffered from poor image quality or complex device structure. The field-emission display (FED) is a cathodoluminescent device that may overcome these limitations. In it, electrons from field-emission cathodes on one substrate excite phosphor anode regions on another. Each cathode is made up of multiple (typically up to thousands) microscopic field-emission tips fabricated on a common substrate using integrated circuit techniques. Four FED design approaches are investigated and compared in this work.

The proximity-focused approach is considered first. This is the arrangement used in the earliest FED prototypes [1]–[3]. A red-green-blue picture element ("RGB pixel") consists of adjacent red, green and blue sub-pixels and is illustrated in Fig. 1. The maximum pixel density is limited by the size of the electron beam at the anode in order to avoid unintentional excitation of adjacent phosphor regions ("mislanding"). The anode must be kept in close proximity to the cathodes (typically 0.1–0.5 mm) in order to achieve pixel densities useful for television and personal computer displays (2–4 pixels/mm). This in turn limits the maximum anode voltage (typically 100–1000 V) that can be used. The switched-anode approach used to demonstrate full-color FED's [4] is considered next. Mislanding is not a concern because the anode potential is multiplexed between the phosphor regions so that only one color is activated at a time. Pixel density is fixed by the phosphor pattern defined on the anode and the maximum anode voltage is limited by the possibility of electrical breakdown between adjacent phosphor regions. The maximum anode voltage of both of the above approaches is much lower than that used for the color CRT's in televisions and personal computers (tens of kilovolts) and requires the use of low-voltage phosphors. The implications on display performance include low luminance, reduced color gamut, short life and limited phosphor selection [5]. These are significant issues that motivate the development of new low-voltage phosphors.

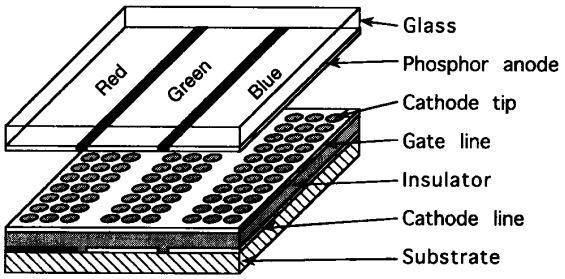

Fig. 1. Proximity-focused field-emission display color picture element ("pixel"). A striped phosphor arrangement is shown, but other arrangements are possible. The anode is typically in close proximity to the cathode substrate (100–500 μm). The cathode pixel consists of three sub-pixels, each servicing a separate red, green or blue phosphor region and being composed of an array of individual emitters. The emitters are typically about a micron wide and separated by five or ten microns.

One possibility for using proven CRT phosphors is to focus the emitted beams so that the anode-cathode separation and voltage can be increased without reducing pixel density. The remaining two approaches considered in this paper supplement the proximity-focused approach with a focus electrode. The aperture-focused approach illustrated in Fig. 2 has long been considered a possibility. Previous computer experiments suggest its effectiveness as a focusing technique [6]–[8]. It is expected to allow greater pixel densities and higher anode voltages at the expense of increased fabrication complexity, larger gate capacitance and higher drive voltage than the proximity-focused approach. The concentric focus electrode illustrated in Fig. 3 is a modification of previous proposals [9], [10] to allow closely-spaced cathode tips, a practical

Manuscript received May 4, 1994; revised July 30 1994. The review of this paper was arranged by Associate Editor J. A. Dayton, Jr.

The authors are with the Department of Electrical and Computer Engineering, University of California, Davis, CA 95616 USA.

IEEE Log Number 9407527.

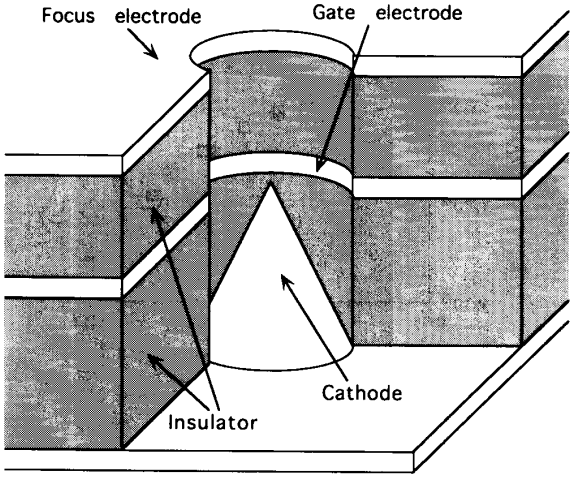

Fig. 2. Cutaway view of an aperture-focused field-emission tip. Electrons are extracted from the cathode by the gate electrode and focused by the aperture lens formed by the focus electrode. The cathode is immersed in the field of the lens, causing some interaction between the emission and focusing mechanisms. Typical cathode height and gate aperture diameter are on the order of a micron.

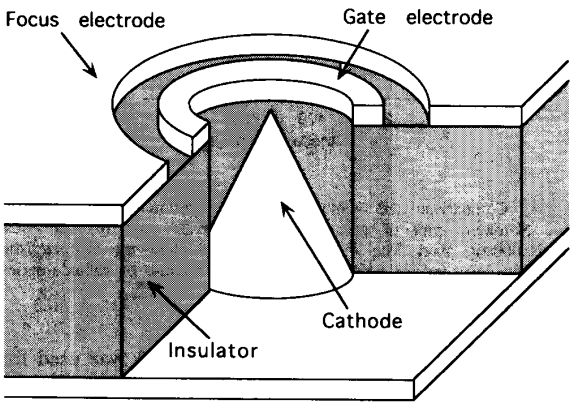

Fig. 3. Cutaway view of a field-emission tip with a concentric focus electrode. The focusing field has little effect on the emission characteristic of the tip, which is dominated by the gate electrode.

requirement in flat-panel displays to minimize the peak-to-peak gate-cathode drive voltage.

II. Method

A commercial finite element software package [11] is used to solve for the electric field in the modeled devices. The finite element approach is particularly well suited for the study of microfabricated field-emission devices because the numerical mesh density can be selectively increased in critical regions and near small geometry's such as the cathode tip, allowing accurate solution without unreasonable computational effort. In addition, complicated electrode geometry's can be accurately represented because mesh nodes are not constrained to lie on a regular grid. For typical cathodes having tip radii of a few tens of nanometers, finite element node spacing on the surface is normally less than one nanometer. Space charge effects within the beam are negligible at the current densities anticipated for display applications [12], so the field solution can be found independently of electron trajectories. We chose to develop our own code for determining electron trajectories and device currents in order to have a full understanding of the approximations and limitations inherent to the results [13]. The field-emission current density is calculated from the Fowler-Nordheim equation at specific points along the surface of the cathode. These points coincide with the locations of finite element nodes used in the field solution. The current corresponding to each point is determined from the product of the Fowler-Nordheim current density and the surface area between points. Trajectories originating at these points are calculated using a fourth-order finite difference integration of the electron equations of motion. Trajectories are not calculated for points emitting negligible current (less than 0.01% of the maximum trajectory current). Integration step size is adaptively adjusted to control local truncation error. Field values between nodes of the finite element mesh are quadratically interpolated. Further than 0.1 mm from the cathode, the trajectories are determined from the exact solution to the equations of motion for electrons in a uniform electric field. The assumption of a uniform field is reasonable for proximity and focused displays since the electrons are far from the cathode and the entire anode substrate is nearly an isopotential surface. Electrode currents and beam width are found from the trajectories. Using a modern RISC workstation, an entire simulation can be completed and graphical output obtained in minutes. This emission model is useful for determining certain directly-observable properties such as operating voltages, currents and beam widths. Insight into finer physical details such as actual emission area and atomic-scale variations is not provided.

The peak emission current required in cathodoluminescent displays depends on display luminance, anode potential, phosphor efficiency and other factors such as face plate optical transmission. For a 1000-line FED with luminance of several hundred candelas per square meter and worst-case assumption for other factors, we estimate the peak cathode current density required for fully "on" pixels to be about 1.5 mA/mm^2. This is less than an average of 50 nA/tip for cathode tips spaced five microns apart. A dark-ambient contrast ratio of 100:1 and a 1000:1 multiplexing ratio for line-at-a-time addressing indicates an "off" current of no more than 0.5 pA/tip on average. The required cathode-gate drive voltages are determined from these currents using the simulated current-voltage characteristics of the devices.

The width of an optical pixel ("spot size") is predominantly determined by the width of the electron beam which excites it. (Optical scattering or internal reflections in the display screen can be factors in some cases.) Since phosphor luminance is proportional to the impinging current density over a wide range, the spot size can be determined from the width of the current density profile of the electron beam. The sub-pixel electron beam is really a composite of beams from individual cathode tips, so the sub-pixel beam width can be found by superimposing the current density profiles of the individual beams. We have found that a good approximation to the sub-pixel beam width is had over a wide range of widths and tip

spacings for these field emitters by adding the width of an individual beam to the width of the sub-pixel at the cathode. (This is not a reasonable approach for Gaussian beams such as occur in CRT's, but the tails of these field-emission beams decay much more rapidly.) Beam width is taken as the full width of the electron beam at 1% of the maximum current density amplitude. Maximum pixel density is taken to be where the sub-pixel beams begin to overlap on the anode. The full pixel width is about three times the sub-pixel width. (If a guard band between sub-pixels is included, the factor is slightly larger than three; if the phosphor is arranged in dot triads instead of stripes, the factor may be somewhat less.)

Electrical breakdown is an important consideration in field-emission flat-panel displays. The maximum operating voltages should be well below device breakdown voltages to ensure reliability. Vacuum breakdown is the main limitation on the anode voltage in proximity and focused designs (assuming that spacers and edge sealing are implemented appropriately). Vacuum field strengths greater than 10^7 V/m are possible in carefully prepared devices, but a practical value for commercial FED's might be closer to 4×10^6 V/m. Using this rule of thumb, an anode gap of 0.1 mm corresponds to a maximum anode voltage of 400 V. We use these anode conditions for modeling the proximity and focused approaches. (Switched-anode FED's have a more severe constraint on maximum anode voltage imposed by the possibility of electrical breakdown between phosphor regions on the screen.) The efficient, high-voltage CRT phosphors used in television and computer displays are non-conductive and are covered with a thin layer of aluminum to serve as the anode. The thinnest aluminum layer that can be inexpensively and reliably applied in the mass production of large display screens requires a minimum anode voltage of about four kilovolts for electron penetration. At a maximum vacuum field strength of 4×10^6 V/m, this corresponds to a minimum anode-cathode gap of one millimeter.

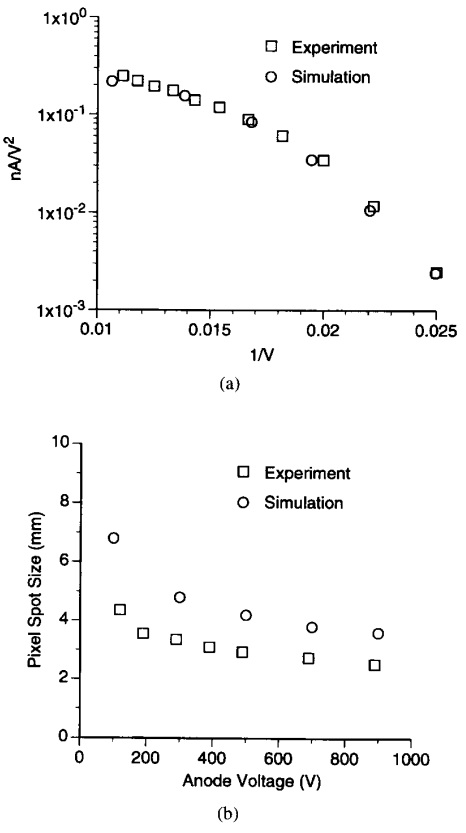

Fig. 4. Comparison of simulated and experimental results: (a) Fowler-Nordheim plot of gate drive characteristic, and (b) spot size of a 10,000-tip pixel. The F-N data does not show the characteristic straight-line behavior for field-emission devices because of cathode series resistance.

III. Verification

Both analytic and experimental verification of the simulations have been obtained. Analytically, simulation results have been verified from conservation of energy considerations and by comparison to the exact solution for infinite parallel plates. By conservation of energy, the kinetic energy of electrons as they impact an electrode should equal the potential energy lost in transit to the electrode. Trajectories calculated for a typical proximity-focused device satisfied this requirement to within a fraction of a percent. Small inaccuracies in the electric field solution near the axis of symmetry caused the trajectory lying along the axis to have an energy error of up to 5%. We are able to accept the error since resulting beam widths and electrode currents are mainly dependent on trajectories far from the axis of symmetry. Trajectories were also modeled between parallel plates. The impact positions and transit times matched the exact solution to better than 0.01%. A tighter local error bound can be specified for the simulation if greater accuracy is required, but this increases computational time and is not necessary for our analysis. A plate separation of 0.1 mm (typical for a proximity-focused FED) was used for the parallel plate verification. Initial electron velocity was 10 eV and plate voltage was 10 V, both lower than the typical operating conditions for FED's but chosen to exaggerate the global error of the trajectory integration. Plots of modeled and exact trajectories are indistinguishable.

Experimental verification of our simulation techniques relied on data provided by LETI, a research group within the French Atomic Energy Commission. Gate drive characteristics and beam widths for proximity-focused cathodes were calculated and compared favorably with the experimental results, as shown in Fig. 4. The device geometry and dimensions were estimated from electron micrographs. The cathode work function and insulator permitivity were determined from device materials. The cathode series resistance and field-enhancement factor were found by matching the calculated gate drive characteristic to experimental data. The experimental and calculated gate drive characteristics are compared for a single proximity-focused cathode tip in Fig. 4(a). Anode spot sizes due to a single cathode tip were then calculated and found to be about a factor of two smaller than the single-tip experimental data. The calculated spots are circular with smooth intensity profiles due to the simple model being used for the cathode

surface (smooth surface with uniform work function). Actual devices emit clusters of sub-spots, suggestive of nanoscopic surface irregularities [14]. This difference is not critical to the engineering analysis being done here. The calculated spot size of an individual proximity-focused cathode tip was used to approximate the spot size of a full sub-pixel composed of 10,000 tips. The results are plotted in Fig. 4(b) against further experimental data on a 1 mm^2 cathode composed of 10,000 tips. Calculated pixel spot sizes are about a factor of two larger than experiment in this case. The difference could be partly due to neglecting tip-to-tip variations. Interaction between tips is not expected to be significant at this tip density. The modeled results mirror the experimental trend toward smaller spots with higher anode potentials.

IV. Results

A. Proximity Focus

The geometry of Fig. 5 was used for the gated cathode in this analysis. The cathode is a 0.65 μm high cone having a 78° apex angle and a spherical tip with 20 nm radius. The gate is 0.2 μm thick with a 1.05 μm diameter aperture centered on the cathode tip and resting on a 0.55 μm layer of insulator. A relative permitivity of 3.9 is used for the insulator to model silicon dioxide. This geometry is representative of typical gated field-emission structures. The geometry of any actual devices will vary somewhat with design and fabrication techniques. The calculated current-voltage characteristic of the device is plotted in Fig. 6. The anode voltage has very little effect on the gate drive characteristic in most display applications because the anode is hundreds of times farther from the cathode tip and exerts minimal influence over emission. Taking 50 nA/tip as the peak white current, the peak white voltage is found from Fig. 6 to be 75 V. The black voltage does not need to be zero to turn a pixel off, but only low enough to reduce the black current to an acceptably low level. This level is determined by the required contrast ratio of the display and the multiplexing ratio used to address the lines. For a 1000 line display with 100:1 contrast ratio, the black current is five decades below the peak white current, corresponding to a black voltage of 40 V. The drive voltage is therefore 35 V peak-to-peak. The cathode tip is centered in the gate opening, so electrons emitted at the tip are not intercepted by the gate as they accelerate toward the anode. Real devices demonstrate a small amount of gate current, presumably due to irregularities on the sides of the cathode which act as emission sites much as the tip itself does. This current is negligible since the capacitive gate current is far more significant in matrix-addressed displays.

Electron trajectories calculated for typical operating conditions are shown in Fig. 5. Each trajectory is launched from a unique position on the cathode surface and carries the amount of current emitted from that area of the surface. These currents, along with the positions at which the trajectories impact the anode, give the anode current density profile plotted in Fig. 7. Due to the rapid decay of the profile tails, the anode beam width is not critically sensitive to the height at which it is measured. For example, the beam width at 1% of the maximum amplitude is only slightly different than that at 0.01%. Emission from actual tips is concentrated into irregular lobes [14] but this does not appear to affect the overall beam width. Single-tip beam width is plotted as a function of anode-to-cathode spacing in Fig. 8(a). Display resolution can be estimated from the beam width of a single emission tip as follows. An RGB pixel is composed of at least one red, green and blue sub-pixel and is therefore about three times larger than the sub-pixel. Each sub-pixel is made up of an array of closely spaced emitters and its spot size is estimated by superimposing the beam profiles of the individual emitters. The pixel size at the anode is roughly $3(s + nd)$, where s is the beam width from Fig. 8(a) and nd is the width of the cathode sub-pixel. The sub-pixel is n tips wide with distance d between tips. Resolution is the inverse of pixel size and is plotted against anode-cathode spacing in Fig. 8(b) for the case of 50 μm wide cathode pixels. Conventional direct-view television requires at least 25 pixels per inch. Computer, military and next-generation television displays require higher resolutions. The maximum anode-cathode spacing and voltage of proximity-focused FED's are severely limited in such applications.

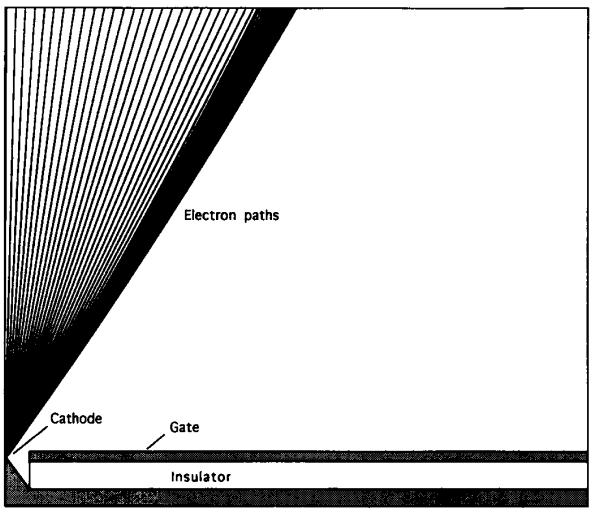

Fig. 5. Proximity-focused field-emission tip and calculated electron trajectories. Due to cylindrical symmetry of the device being considered, only one half of a cross sectional view is shown. The gate and anode voltage for this calculation were 75 and 400 volts, respectively, with respect to the cathode.The total emission current is 50 nA. The region shown is 10 μm high; the anode is 100 μm away and is not shown in this view. The trajectories launched from the side wall of the cathode cone tend to bunch at the edge of the beam, but carry very little current.

B. Switched Anode

Unlike the proximity-focused approach, switched-anode devices have only a single cathode pixel for the RGB anode pixel. Each cathode pixel provides electrons for the red, green and blue phosphor regions, one at a time. High-resolution displays require high pixel density and a small distance between the red, green and blue regions. This reduces the maximum anode voltage that can be used without causing electrical breakdown

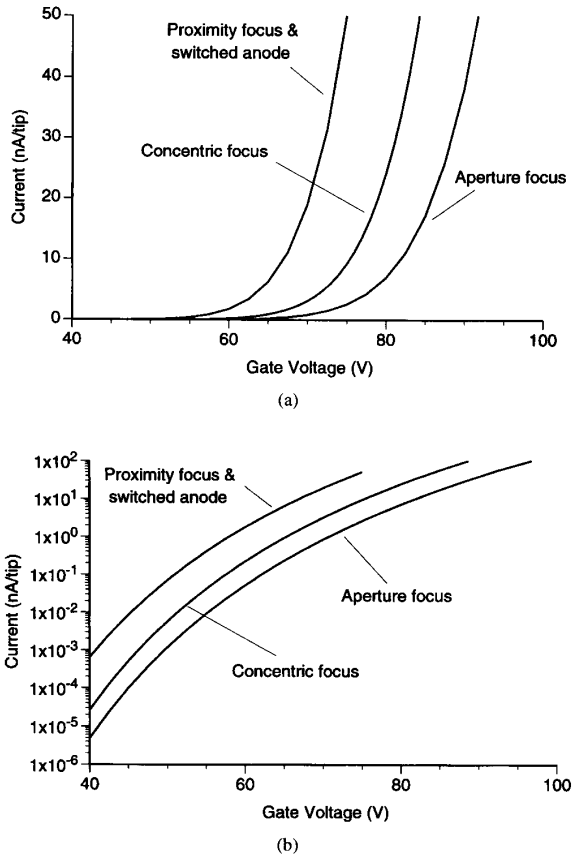

Fig. 6. Calculated gate drive characteristics for the devices being considered. A linear current scale is conventional (a), but the logarithmic scale of (b) is more useful for determining peak-to-peak drive voltages in display applications. The cathode is at reference potential. Lowest turn-on and peak-to-peak gate voltages are possible with the proximity-focused device.

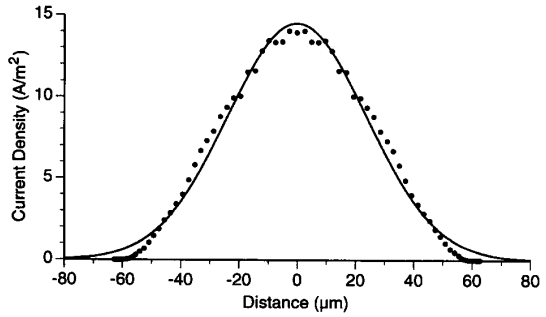

Fig. 7. Calculated current density at the anode due to a single proximity-focused field-emission tip. The best-fit Gaussian curve is also shown. The non-smooth nature of the data is an artifact of the computational techniques. The current density profiles of experimental devices are much less smooth due to surface irregularities in real devices, but the overall distribution widths are comparable. An anode spacing of 0.2 mm and potential of 800 V were used for this calculation, corresponding to typical operating conditions.

between the separate regions. The gate drive characteristics of switched-anode and proximity-focused devices are similar since the differences in anode structure have a small affect

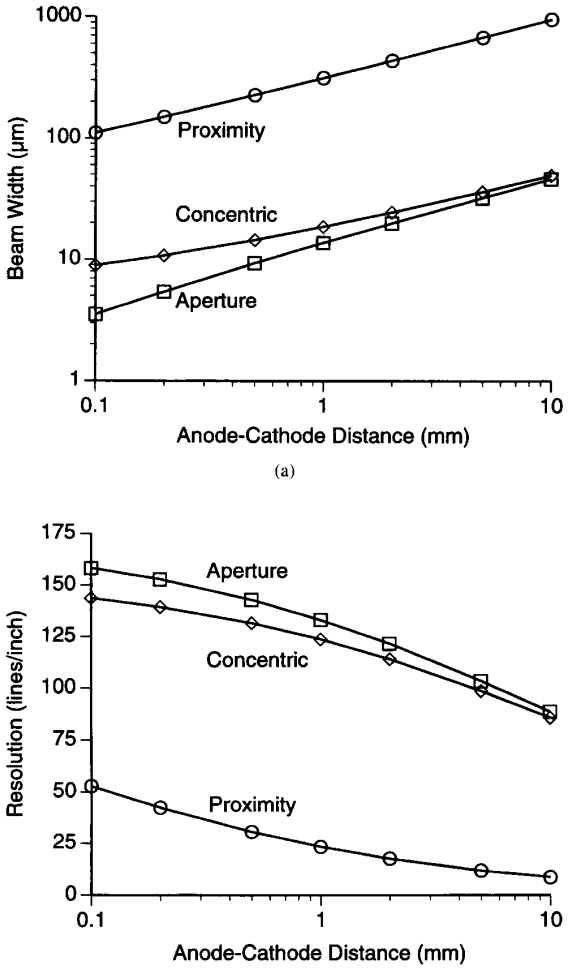

Fig. 8. (a) Single-tip beam widths and (b) display resolution as a function of anode spacing. Beam current is 50 nA and cathode sub-pixels are 50 μm wide in all cases. The anode potential was varied with anode spacing to maintain a maximum field strength of 4 kV/mm in the region between the anode and cathode substrates. Relativistic effects are minor over the range of acceleration voltages considered here.

on the electric field near the field-emission tips. Net anode current may be smaller in switched-anode devices, however, since some current escapes the active region of the anode and falls back on the gate. This is demonstrated by the calculated trajectories of Fig. 9. The geometry of Fig. 9 is based on an abstraction of the switched-anode geometry and is unrealistic for use in real displays, but it clearly demonstrates the origin of gate current and the excitation of individual phosphor regions. As expected, beam mislanding is negligible because electrons can only land on the electrically selected phosphor.

C. Aperture Focus

Aperture-focused tips are investigated by adding additional layers of insulator and metal to the proximity structure. Figure 10 shows simulated electron trajectories for a prototype geom-

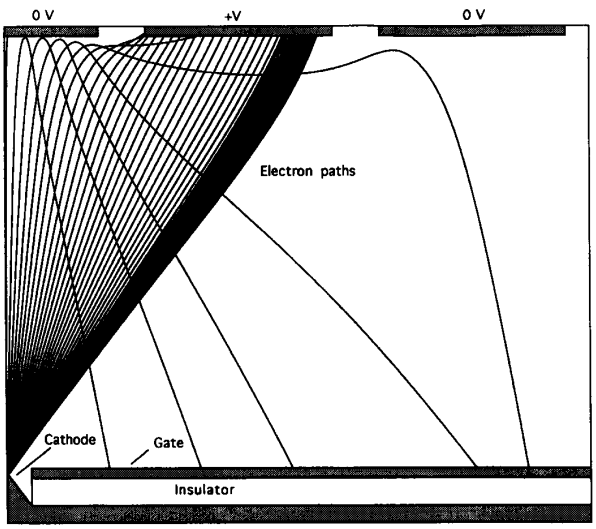

Fig. 9. A simplified switched-anode device showing calculated electron trajectories when one phosphor region is connected to anode potential. The high gate current in actual switched-anode devices can be seen to be caused by electrons that escape the active anode region and "fall" back to the gate. Real switched-anode devices have substantially larger anode regions that are serviced by an array of field-emission tips simultaneously.

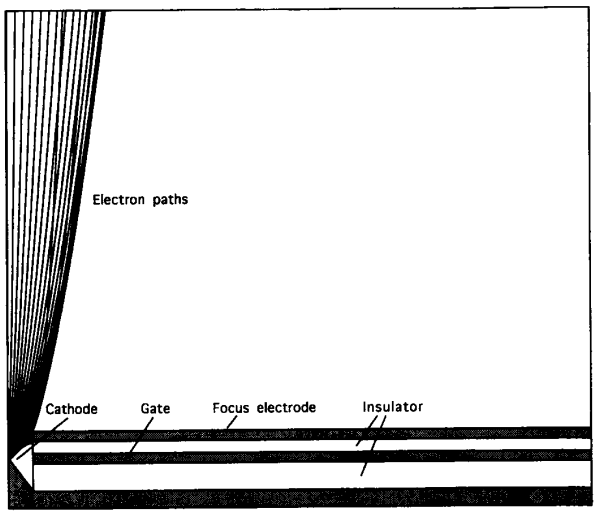

Fig. 10. Close-up view of an aperture-focused field-emission tip and simulated electron trajectories. The gate, focus electrode and anode potentials were 92.5, 4.5 and 400 volts positive with respect to the cathode, respectively. The anode was 0.1 mm from the cathode and the total emission current was 50 nA. Electron velocity is reduced in the vicinity of the focus electrode when this electrode is biased near the cathode potential as shown here, allowing electrons to be deflected toward the anode. Some electrons are typically intercepted by the focus electrode.

etry and typical bias conditions. The gate drive characteristic is plotted alongside the proximity-focused curve in Fig. 6 for a device with the focus electrode placed 0.75 μm above the gate electrode. Some of the emission current is intercepted by the focus electrode and insulator before it reaches the anode but this has been kept below 5% by increasing the diameter of the focus aperture to 2 μm. The current intercepted by the insulating layer between the gate and focus electrodes will only be transient unless the dielectric has high surface conductivity. We anticipate that the nature of the insulator surface, and in particular its conductivity, can be adequately controlled by the fabrication technology to avoid surface charging. The gate drive curve of Fig. 6 reveals that higher gate voltages are required than for the proximity-focused device. This is due mainly to the fact that the focus electrode is biased near the cathode potential and detracts from the electric field strength produced by the gate at the emitter tip. A secondary cause of the increased drive voltage is interception of some of the emitted current. For a 1000 line display with 100:1 contrast ratio and a peak white current of 50 nA/tip, the aperture-focused structure is found to require a gate drive of about 50 $V_{p\text{-}p}$ when highly focused, verses 35 $V_{p\text{-}p}$ found for the proximity-focused structure. From a practical standpoint, this is potentially serious because above about 40 $V_{p\text{-}p}$ the integrated circuits required to drive the rows of the display become significantly more expensive. Increasing the spacing between the focus electrode and the gate reduced the drive voltages somewhat, but spacings much beyond one micron result in excessive current interception and large beam widths. Reducing the spacing resulted in even higher drive voltages. The maximum voltage between the focus and gate electrodes or the gate electrode and the cathode interconnect is determined by the dielectric strength of the insulating material between them (usually an oxide or nitride of silicon). The bulk breakdown field strength of thermally grown silicon dioxide is about 600 V/μm. Deposited silicon dioxide has a relatively lower dielectric strength that depends on the deposition and annealing processes, but is still sufficient for practical devices and is commonly used for many types of microfabricated field-emission cathodes.

Aperture-focused beam width and prototypical resolution are plotted as a function of anode distance for a fixed focus potential in Fig. 8. Smaller beams can be obtained by choosing the optimum focus voltage for each anode distance. The variation in beam width with gate voltage is small for a fixed focus bias, suggesting that DC focus bias which would significantly simplify the support electronics may be adequate for display applications.

D. Concentric Focus

A focusing structure which has the focus electrode in the same plane as the gate is shown in Fig. 3. Designs with multiple concentric electrodes have been considered before, but do not appear practical for flat-panel displays because of their large surface area. The calculated gate drive characteristic is plotted in Fig. 6. Gate and focus electrode currents are found to be zero. As with the proximity-focused device, a small amount of gate current is expected in real devices due to emission from the cathode walls. The focus electrode is negatively biased and will truly intercept no current in actual devices. The peak-to-peak swing for a 1000-line display with 100:1 contrast ratio is just under 40 volts. This is higher than the proximity-focused result but a good improvement over the aperture-focused structure. The drive characteristic is quite

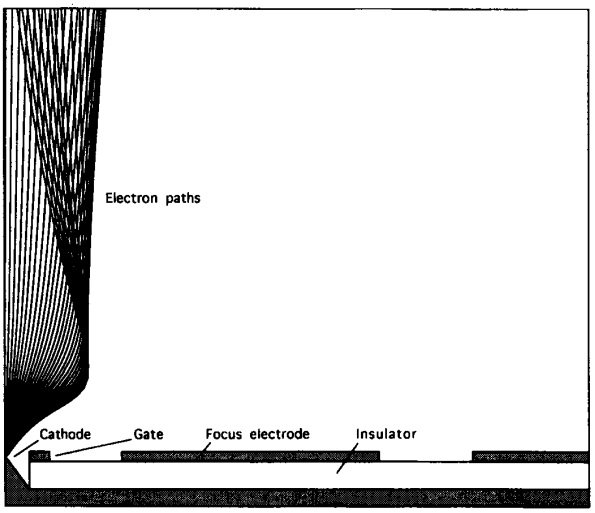

Fig. 11. Close-up view of a field-emission tip with concentric gate and focus electrodes. The gate, focus electrode and anode potentials with respect to the cathode were 82.5, −20 and 380 volts, respectively. The anode was 0.1 mm from the cathode and total emission current was 50 nA. The focusing field does not penetrate significantly to the cathode tip, minimizing the effect of the focus electrode on emission current.

insensitive to the focus electrode bias and geometry since the tip is shielded by the gate. Figure 11 shows calculated electron trajectories for a well-focused beam.

This design offers many benefits over the aperture-focused design: reduced gate capacitance and current, lower gate drive voltages, and potentially simplified fabrication. Still, a potential drawback is evident: the electric field strength between the gate and focus electrodes can be high enough to initiate breakdown unless tip-to-tip spacing is increased to allow more distance between these electrodes. To investigate this concern, we increased the gap between the gate and focus electrodes from 2 to 5 μm. The optimum focus voltage increased by only 25% (from −20 to −25 V), resulting in a net reduction in field strength between the electrodes by a factor of two. There was no significant effect on either the drive characteristic or the minimum beam width. This suggests that an acceptable margin between operating voltages and electrical breakdown can be obtained by increasing the distance between the concentric electrodes as required. At the same time, it should be kept in mind that in display applications a limitation is imposed by the need to maintain a high density of emitting tips. The peak emission current per tip must increase as the inverse of the square of tip-to-tip spacing in order to maintain peak display luminance. The peak-to-peak drive voltage of the simulated concentric devices increased by almost 10 V as tip-to-tip spacing increased from 5 to 20 μm. In addition to the effect on drive voltage, neighboring tips interact in a way that may affect beam focusing. We modeled the effect of neighboring tips by placing additional concentric electrodes outside the focus electrode. These electrodes were biased at the gate potential to create a worst-case model for tip-to-tip interaction. We found that the effect on beam width is significant, but that the original widths could be reclaimed by

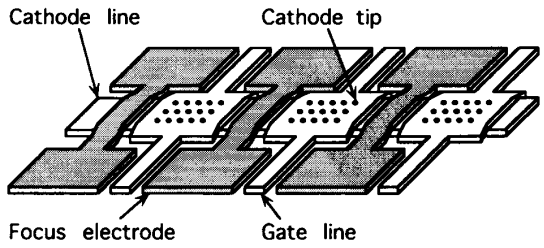

Fig. 12. A pixel-focusing concept which allows high tip density and simple fabrication.

increasing the focus voltage. The drive characteristic and beam width were unchanged from those of an isolated tip when the optimum focus voltage was increased from −20 to −40 V_{dc}. Focus voltage will in fact increase less than this worst-case model suggests.

Beam width and resolution for the concentric design are shown in Fig. 8 and appear similar to those of the aperture-focused case, but a comparably sized pixel contains fewer tips because of the additional surface area required by the concentric electrodes. A possible solution to this limitation is shown in Fig. 12 in which the focus electrodes surrounding each tip are replaced by electrodes encircling each sub-pixel as a whole. For large anode-cathode spacing, the area used by these electrodes is otherwise wasted to allow for divergence of the beams in transit to the anode. Implementing the electrodes in this manner allows tips to be placed much more closely together to increase operational life, improve luminance uniformity and reduce drive voltages. Manufacturing yield is also expected to be higher due to simpler lithography.

V. Conclusion

Proximity-focused and switched-anode field-emission displays have been demonstrated in recent years, but the maximum anode voltage has been limited to less than one kilovolt. This is too low for the commercially available phosphors now used in color CRT's and requires the use of low-voltage phosphors which currently demonstrate lower efficiency, inferior color saturation and generally poorer performance. The maximum resolution of proximity-focused devices operating at anode voltages consistent with CRT phosphors (above about 4–5 kV) is found to be 1 line/mm (25 lines/inch). This situation may improve somewhat as tip reliability and tip-to-tip uniformity improve and allow fewer tips to service smaller pixels, but resolution in the near term is likely to remain inadequate for the requirements of modern computer displays and next-generation television. Focusing the electron beams from field-emission cathodes could allow greater anode-cathode spacing without loss of resolution, permitting higher anode voltages and proven CRT phosphors.

Two focused designs have been shown to yield exceedingly small beam widths (on the order of 10 μm, even at anode distances exceeding 1 mm, which could support several kilovolts of potential drop). Resolutions exceeding 4 lines/mm (100 lines/inch) are compatible with the large anode spacings and high anode voltages needed for CRT phosphors.

This is significant because such resolutions are generally inaccessible to conventional color CRT's and impractical for liquid crystal displays. A design using an aperture electrode parallel to the gate electrode on the cathode substrate for beam focusing achieved good focusing properties and acceptable dielectric stress, but the gate drive voltage was found to increase significantly (≈30%) over the proximity-focused case. A concentric electrode design, in which the focus electrode lies in the same plane as the gate electrode and surrounds each emission tip, demonstrated similar improvements in beam width and only about 15% increase in drive voltage. The lower drive voltages, capacitance and current should allow for low-power row and column drive circuits. Fabrication is also relatively simple in that the focus electrode can be defined in the same metal layer as the gate. These are significant advantages that may eventually allow the use of well-proven CRT phosphors in field-emission displays. Implementing the concentric electrode around each sub-pixel instead of each tip might enhance the performance further. Modeling this concept in two dimensions is expected to be adequate for guiding prototype design efforts, but full three-dimensional analysis may be required for refining design details. Experimental examples are now required to optimize these focused designs for flat-panel display applications. Cathode-anode spacer technology must also be developed further before such designs can become fully practical.

ACKNOWLEDGMENT

The authors wish to thank Robert Baptist, Christophe Py, and F. Levy of the French Atomic Energy Commission's LETI laboratory for providing the experimental data used to verify our simulation techniques. Thanks are also extended to Ivor Brodie of SRI International for helpful suggestions.

REFERENCES

[1] R. Meyer, A. Ghis, Ph. Rambaud and F. Muller, "Microtips fluorescent display," *Proc. 6th Int. Display Research Conf., Society for Information Display*, pp. 512–515, 1986.
[2] C. A. Spindt, C. E. Holland, I. Brodie, J. B. Mooney, and E. R. Westerberg, "Field-emitter arrays applied to vacuum fluorescent display," *IEEE Trans. Electron Devices*, vol. 36, pp. 225–228, 1989.
[3] R. Meyer, "6 diagonal microtips fluorescent display for T.V. applications," *Proc. 10th Int. Display Research Conf.*, Society for Information Display, pp. 374–377, 1990.
[4] R. Meyer, "Recent developments on "microtips" display at LETI," *Technical Digest 4th Int. Vacuum Microelectronics Conf.*, Japan Soc. Applied Physics, pp. 6–9, 1991.
[5] A. G. Chakhovskoi, W. D. Kesling, J. T. Trujillo, and C. E. Hunt, "Phosphor selection constraints in application of gated field-emission micro-cathodes to flat-panel displays," *J. Vac. Sci. Technol.*, vol. B12, pp. 785–789, 1994.
[6] W. B. Herrmannsfeldt, R. Becker, I. Brodie, A. Rosengreen, and C. A. Spindt, "High-resolution simulation of field emission," *Nuclear Instruments and Methods in Physics Research*, vol. A298, pp. 39–44, 1990.
[7] R. M. Mobley and J. E. Boers, "Computer simulation of micro-triode performance," *IEEE Trans. Electron Devices*, vol. 38, pp. 2383–2388, 1991.
[8] W. D. Kesling and C. E. Hunt, "Field emission display resolution," *Soc. Information Display Int. Symp. Digest*, pp. 599–602, 1993.
[9] C. A. Spindt, "Automatically focusing field emission electrode," U.S. patent 4,874,981, 1989.
[10] T. Leroux and C. Py, "Système permettant de maîtriser la forme d'un faisceau de particules chargées," French patent 92403558.7, 1992.
[11] "Maxwell 2-D field simulator," Ansoft Corporation, Pittsburgh.
[12] I. Brodie and C. A. Spindt, "Vacuum microelectronics," *Advances in Electronics and Electron Physics*, vol. 83, pp. 1–106, 1992.
[13] W. D. Kesling and C. E. Hunt, "Field emission device modeling for application to flat panel displays," *J. Vac. Sci. Technol.*, vol. B11, pp. 518–522, 1993.
[14] C. Py and R. Baptist, "Stability of the emission of microtips," *Tech. Digest 6th Int. Vacuum Microelectronics Conf., IEEE*, pp. 23–24, 1993.

W. Dawson Kesling (S'92) received the B.S. degree in electrical engineering from the University of California, Los Angeles, and the M.S. degree in the same field from the University of California, Berkeley. Between 1986 and 1991, he held engineering positions at Apple Computer contributing to the development of high-resolution personal computer displays. Since 1991, he has been a Ph.D. student and research assistant at the University of California, Davis, where his research interests center on the application of microfabricated field emitters to flat-panel displays. He is a student member of the Society for Information Display.

Charles E. Hunt (S'78–M'80–S'80–M'86–SM'94) received the B.S.E.E. and M.S.E.E. degree from the University of Utah, Salt Lake City, UT, and the Ph.D. degree in electrical engineering from Cornell University, Ithaca, NY. From 1979 to 1983 he served as Staff Engineer to the VLSI Design Research Group in the Computer Science Department of the University of Utah, working on structured logic design and testing. Since 1986, he has been with the Department of Electrical and Computer Engineering at the University of California at Davis, where he is an Associate Professor, as well as a Staff Consultant for the Engineering Research Division of the Lawrence Livermore National Laboratory. Professor Hunt teaches IC fabrication technology and semiconductor device physics. His research centers on microfabrication technology and process design for electronic materials, electronic devices and circuits, and microstructures.